

Received November 16, 2019, accepted December 16, 2019, date of publication December 24, 2019, date of current version January 23, 2020.

Digital Object Identifier 10.1109/ACCESS.2019.2961939

Indoor Real-Time 3-D Visible Light Positioning System Using Fingerprinting and Extreme Learning Machine

YIRONG CHEN¹, WEIPENG GUAN², JINGYI LI³, AND HONGZHAN SONG³

¹School of Electronic and Information Engineering, South China University of Technology, Guangzhou 510640, China

²Department of Information Engineering, The Chinese University of Hong Kong, Hong Kong

³School of Automation Science and Engineering, South China University of Technology, Guangzhou 510640, China

Corresponding author: Weipeng Guan (gwpscut@163.com)

This work was supported in part by the National Undergraduate Innovative and Entrepreneurial Training Program under Grant 201710561006 and Grant 201810561083, and in part by the Special Funds for the Cultivation of Guangdong College Students' Scientific and Technological Innovation (Climbing Program Special Funds) under Grant pdjh2017b0040 and Grant pdjha0028.

ABSTRACT Photodiode-based (PD-based) visible light positioning (VLP) has become a research focus of indoor positioning technology, while the existing VLP models rarely consider the anti-interference and positioning time of that. In this paper, indoor real-time three-dimensional visible light positioning system using fingerprinting and extreme learning machine (ELM) is proposed to make the system achieve not only high positioning accuracy and elevated anti-interference but also well-behaved real-time ability. In contrast to the positioning system based on K-Nearest Neighbor or Support Vector Machine, the proposed system achieves the highest positioning accuracy and the state-of-the-art positioning speed. Furthermore, the visible light positioning kernel is proposed as a method to reduce the size of the fingerprint database and thus reduce the training time exponentially. Both the simulation and the experiment results show that the proposed system achieves real-time 3-D positioning with high anti-interference. Therefore, this scheme can be considered as one of the effective methods for indoor 3-D positioning.

INDEX TERMS Extreme learning machine (ELM), photodiode (PD), positioning fingerprint, real-time positioning, visible light positioning (VLP).

I. INTRODUCTION

With the development of artificial intelligence, indoor applications have become increasingly demanding for positioning services. Performing high-speed indoor positioning on the premise of ensuring accuracy is the basis for service robots and drones to be used in indoor scenes. In the field of positioning, Global Positioning System (GPS) has been widely used outdoors. However, GPS is difficult to work well in indoor environments due to weak radio signal strength and the inability to completely penetrate the walls of buildings and houses [1]. In the field of indoor positioning technology, wireless local area networks (WLAN), infrared, radio frequency identification (RFID), Zigbee, ultra-wide band (UWB) and Bluetooth have been widely studied. However, these positioning technologies have not been widely applied on account

of additional wireless anchors, high cost, slow positioning speed or low positioning accuracy [2]–[4]. Different from the above-mentioned indoor positioning technology, VLP technology is based on visible light communication (VLC). On the one hand, indoor VLP technology does not need to install additional transmitters in the room, only need to change the Light Emitting Diode (LED) driving circuit. On the other hand, the LED-based lighting provides illumination, positioning, and communication at little additional cost [5].

According to the difference of sensors, indoor VLP can be divided into two types: camera-based positioning and photodiode-based (PD-based) positioning [6]–[8]. In the case of camera-based, the indoor positioning system consists of a LED array and the image sensor with high frame rate. This positioning technique requires a stable camera placement, as little jitter as possible [9]. What's worse is that it needs to repeatedly capture images and perform image

The associate editor coordinating the review of this manuscript and approving it for publication was Nianqiang Li.

processing which means that the memory consumption of the system is extremely large and it is difficult to achieve real-time positioning due to the computational complexity. Different from the camera-based positioning technology, PD-based positioning technology obtains the position ID and the received power of the LED through the PD detecting the LED signal. So far, the PD-based positioning technology has been deeply explored, and there are some models to calculate the position of the receiver, such as the angle of arrival (AOA), time of arrival (TOA), time difference of arrival (TDOA) or received signal strength (RSS) [10]. Taking into account of the difficulty, accuracy and cost of indoor positioning, PD-based indoor positioning using RSS algorithm is preferred due to its high accuracy and low cost. Of course, before applying the RSS algorithm, the problem of multiple LEDs transmission signals causing inter-cell interference needs to be solved. Therefore, in our previous study [11], [13], the signal from LEDs installed on the ceiling is modulated in code division multiple access (CDMA) to reduce inter-cell interference caused by the presence of multiple LEDs.

So far, indoor three-dimensional positioning based on VLC focuses more on algorithm research. Heidi Steendam put forward a 3-D positioning algorithm based on AOA and the maximum likelihood principle, achieving an accuracy of 10 cm but with high complexity [12]. In [13], Hao Chen *et al.* proposed a reversed three-dimensional VLC-based positioning system using RSS and genetic algorithm (GA) to realize precise positioning service at high computational costs operation. In [11], Ye Cai *et al.* proposed a 3-D VLC-based positioning system based on the modified particle swarm optimization (PSO) algorithm and RSS with the average error of 3.9 mm, using only when LEDs' luminous power is extremely stable. In [14], DANIEL KONINGS *et al.* developed a VLP system using Convolutional Neural Network-based (CNN-based) wireless localization with the mean error 0.12 m. However, the proposed system was only realized in simulation with no experimental verification. The above-mentioned three-dimensional positioning algorithms all achieve a very high positioning accuracy. However, since the above positioning method involves a high amount of computation, the positioning time is more than 0.1 s and it is difficult to apply to the actual system. Alternately, Bingcheng Zhu *et al.* considered both positioning time and positioning accuracy and proposed a three-dimensional VLC-based positioning algorithm based on the method of exhaustion (MEX). The proposed algorithm achieved an average positioning error of 3.20 cm with a positioning time cost of 0.36 s, thus making challenging to achieve real-time position [15]. Ming Xu *et al.* combined the fingerprint positioning algorithm with the VLP algorithm, and use K-Nearest Neighbor (KNN) algorithm to achieve three-dimensional positioning [16]. The disadvantage of KNN is that the amount of calculation is large, because each sample to be located must calculate its distance to all known samples in order to obtain its K nearest neighbors [17].

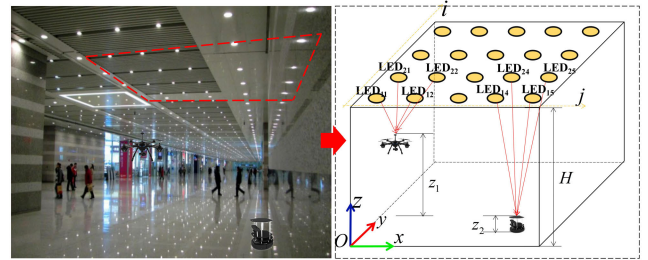


FIGURE 1. Indoor optical wireless positioning system: the left side of the figure is the actual scene, and the right side is the system model.

In this paper, we propose an indoor real-time 3-D VLC-based positioning system using fingerprinting [18], [19] and extreme learning machine (ELM) technology [20]–[22]. The positioning fingerprint is originally applied in the PADAR positioning system [19]. This method effectively avoids the shortcomings of the traditional indoor positioning system relying on a single RF signal. In addition, in 3-D positioning algorithm, the receiving intensity of the PD is affected by both the distance and the angle. Fortunately, fingerprinting positioning is more practical in this case. ELM is a simple and effective single hidden layer feedforward networks (SLFNs) learning algorithm that can obtain the global optimal solution with high learning speed and strong adaptability to new samples, compared with support vector machine (SVM) [22], [23]. Therefore, using ELM and fingerprinting based on VLC can quickly obtain the three-dimensional coordinates of the target point.

The rest of this article is organized as follows. Section II introduced the proposed three-dimensional positioning algorithm in detail. Section III provided positioning accuracy and time in simulated experiment. Section IV provided positioning accuracy and time in real-world experiment. Section V concluded the article.

II. SYSTEM PRINCIPLE AND ALGORITHM

A. INDOOR OPTICAL WIRELESS CHANNEL MODEL

As shown in Fig. 1, a large number of LEDs are installed on the ceiling to meet the lighting requirements. PD receivers are installed on indoor objects such as unmanned aerial vehicle (UAV) and robots to receive signals from LEDs. The absolute coordinates of these LEDs can be represented by $C_{ij} = [X_{ij}, Y_{ij}, Z_{ij}]^T$, ($i = 1, 2, 3, \dots$ and $j = 1, 2, 3, \dots$ is the LEDs' distribution number), respectively. Similarly, the absolute coordinates of different PDs can also be represented by $c_k = [x_k, y_k, z_k]^T$, ($k = 1, 2, 3, \dots$ is the positioning number), respectively. The radiant intensity of a LED is usually assumed to follow a Lambertian radiation pattern. Relation between the received optical power of the PD located at c_k and the emitted optical power of the LED located at C_{ij} can be given as [24]

$$P_{ijk} = P_{ij}^T \frac{A_r(m+1)}{2\pi d_{ijk}} \cos^m(\phi_{ij}) T(\psi_{ijk}) G(\psi_{ijk}) \cos^M(\psi_{ijk}) \quad (1)$$

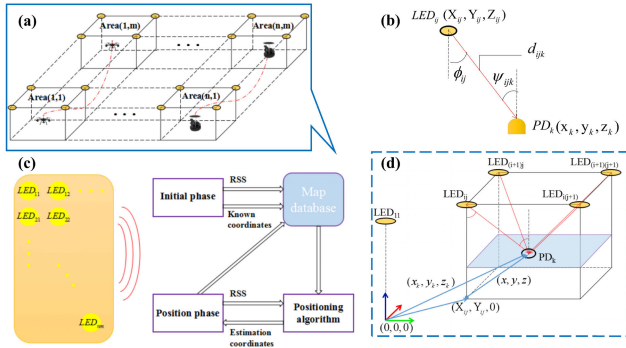


FIGURE 2. VLP using fingerprinting: (a) traditional model for fingerprint positioning, (b) geometric relation between LED and PD, (c) the training process (initial phase) and the positioning process (positioning phase) of fingerprint positioning, (d) VLP kernel: Simplified fingerprint positioning using coordinate transformation.

where P_{ij}^T is the emitted optical power of the LED located at C_{ij} , A_r is the effective area of the PD at the receiver located at the point c_k , $m = -\ln(2)/\ln(\cos(\phi_{1/2}))$ and $M = -\ln(2)/\ln(\cos(\psi_{1/2}))$, where $\phi_{1/2}$ and $\psi_{1/2}$ are the half-power angles of the LED and PD. d_{ijk} is the distance between point C_{ij} and point c_k . ϕ_{ij} is the irradiation angle of the LED located at C_{ij} and ψ_{ijk} the incidence angle of the PD located at c_k .

Geometric relation between LED_{ij} and PD_k is shown in Fig. 2 (b). The distance d_{ijk} between the LED_{ij} located at C_{ij} and the PD_k located at c_k can be calculated as

$$d_{ijk} = \sqrt{(x_k - X_{ij})^2 + (y_k - Y_{ij})^2 + (z_k - Z_{ij})^2} \quad (2)$$

The irradiant angle ϕ_{ij} can be represented as

$$\cos(\phi_{ij}) = \frac{|z_k - Z_{ij}|}{\sqrt{(x_k - X_{ij})^2 + (y_k - Y_{ij})^2 + (z_k - Z_{ij})^2}} \quad (3)$$

Using Equations (1), (2), and (3), we can calculate the c_k theoretically. However, the equation sets for solving (x_k, y_k, z_k) are nonlinear and it is difficult to obtain the precise received optical power due to the interference of ambient light in practical VLP system [11], [14]. This makes the current three-dimensional positioning algorithm less suitable than the fingerprint algorithm in the positioning scene using VLC.

B. TRADITIONAL VLC FINGERPRINTING ALGORITHM

As shown in Fig. 2 (a), $(n + 1) \cdot (m + 1)$ LEDs are mounted on the ceiling in the position area in traditional VLC fingerprinting positioning scene. In the initial phase, the vector of received optical power $P_{k'}$ can be given as

$$P_{k'} = [P_{11k'} \quad P_{12k'} \quad \dots \quad P_{ijk'} \quad \dots \quad P_{(n+1)(m+1)k'}]^T \quad (4)$$

where $P_{ijk'}$ is the received optical power from LED_{ij} at $c_{k'} = [x_{k'}, y_{k'}, z_{k'}]^T$, $k' = 1, 2, \dots, K'$.

In the positioning phase, the vector of received optical power P_k can be expressed as

$$P_k = [P_{11k} \quad \dots \quad P_{ijk} \quad \dots \quad P_{(n+1)(m+1)k}]^T \quad (5)$$

where P_{ijk} is the received optical power from LED_{ij} at c_k .

When $n \geq 1$ and $m \geq 1$, we can use the sampling database to estimate the coordinates of the measured point and control the error to a lower level. However, when the values of n and m increase, the volume of the fingerprint database rapidly increases, and many useless data are generated. For example, there are many elements having a value of 0 in the vector $P_{k'}$ and P_k . These data do not help fingerprint positioning and greatly increase the positioning time.

C. MODIFIED ELM FOR VLP USING FINGERPRINTING

Considering that the existing fingerprint location algorithm is not suitable for scenes with large-scale LEDs, we propose a high-speed, high-accuracy three-dimensional positioning system based on ELM. We creatively propose the concept of a VLP kernel for fingerprinting.

In this positioning system, the positioning concept is divided into absolute positioning and relative positioning according to the coordinate transformation theory. As shown in Fig. 2 (d), the relative positioning refers to using ELM and fingerprint to achieve positioning of the PD, calculating the relative coordinate (x, y, z) of the PD_k with respect to the projection (absolute coordinate: $X_{ij}, Y_{ij}, 0$) of LED_{ij}. Absolute positioning refers to calculating the absolute coordinate of PD_k with respect to the absolute coordinate $(0,0,0)$. Their relationship can be expressed by

$$c_k = [x, y, z]^T + [X_{ij}, Y_{ij}, 0]^T \quad (6)$$

In Equation (6), X_{ij} and Y_{ij} can be obtained through VLC because they are coded and transmitted as LED's position coordinates and the receiving PD can receive them and obtain their values. We can divide the entire positioning space into $m \times n$ subspaces. Each of the four corners of each subspace has one LED installed. Visible fingerprint positioning only needs to be performed in these subspaces. The positioning algorithm in each subspace is the same, so it can be described abstractly as a visible light fingerprint positioning kernel. We only need to use the data of one subspace during the initial phase of fingerprint positioning. Therefore, Equation (4) and (5) can be re-described as

$$P_k = [P_{ijk} \quad P_{i(j+1)k} \quad P_{(i+1)jk} \quad P_{(i+1)(j+1)k}]^T \quad (7)$$

The complete fingerprint database can be defined as

$$[P_1 \quad \dots \quad P_k \quad \dots \quad P_K] \Leftrightarrow [c_1 \quad \dots \quad c_k \quad \dots \quad c_K] \quad (8)$$

Assuming that a set of K' training samples in the visible light fingerprint library are independent of each other, the \tilde{K} ($\tilde{K} \ll K$) hidden neurons and the standard SLFNs are shown in Fig. 3, whose activation function is $h(x)$. If the

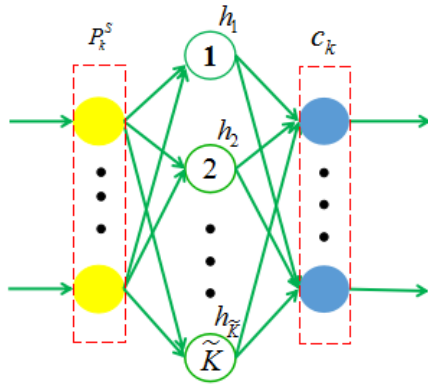


FIGURE 3. The standard single layer feedforward networks.

input data P_k was fed into the neuron network, the estimate positioning coordinate \hat{c}_k can be described as [20]

$$\beta \cdot h(\alpha \cdot P_k + \mathbf{b}) = \hat{c}_k, \quad k = 1, \dots, K \quad (9)$$

where β is the weight matrix of size $3 \times \tilde{K}$ connecting the hidden neurons and output neurons and α is the weight matrix of size $\tilde{K} \times 4$ connecting the input neurons and hidden neurons. $\mathbf{b} = [b_1, b_2, \dots, b_{\tilde{K}}]^T$ is the threshold of the hidden neurons.

Consider the K sampled data together, the corresponding positions can be expressed as [21]

$$\beta \mathbf{H} = \hat{\mathbf{C}} \quad (10)$$

where $\hat{\mathbf{C}} = [\hat{c}_1, \dots, \hat{c}_k, \dots, \hat{c}_K]$ is the output matrix of size $3 \times K$. $\mathbf{H}(\alpha, \mathbf{b}, P_1, \dots, P_K) = [h(\alpha \cdot P_1 + \mathbf{b}), \dots, h(\alpha \cdot P_K + \mathbf{b})]$.

The traditional backward propagation (BP) algorithm learning algorithm requires a lot of time for learning in most cases because it adopts a gradient learning method. Differently, The input weight matrix α and hidden layer threshold \mathbf{b} of the network based on the extreme learning machine do not need to be adjusted during the learning process. Therefore, the least squares solution of (10) can be written as [20]

$$\|\hat{\beta} \mathbf{H}(\alpha, \mathbf{b}) - \mathbf{C}\| = \min_{\beta} \|\beta \mathbf{H}(\alpha, \mathbf{b}) - \mathbf{C}\| \quad (11)$$

where $\mathbf{C} = [c_1 \dots c_k \dots c_K]$ is the ideal output matrix.

The least squares solution of Equation (11) can be expressed as [22]

$$\hat{\beta} = \mathbf{C} \mathbf{H}^\dagger \quad (12)$$

where \mathbf{H}^\dagger is the Moore-Penrose generalized inverse matrix of \mathbf{H} . Using orthogonal projection, \mathbf{H}^\dagger can be described as

$$\mathbf{H}^\dagger = \begin{cases} (\mathbf{H}^T \mathbf{H})^{-1} \mathbf{H}^T, & \mathbf{H}^T \mathbf{H} : \text{Non-singular matrix} \\ \mathbf{H}^T (\mathbf{H} \mathbf{H}^T)^{-1}, & \mathbf{H} \mathbf{H}^T : \text{Non-singular matrix} \end{cases} \quad (13)$$

In the actual VLC-based positioning process, we need to consider that collecting samples is very difficult. In order to reduce the number of samples, we can let the positioning system continue learning after initialization [25]. This will reduce the difficulty of training and the difficulty of data

Algorithm 1 VLP system based on ELM

```

1: Step 1. Initialization of ELM
2: Input:  $S = \{(P_k, c_k) | k = 1, 2, \dots, K\}$ 
3: Random number generator: generate  $\alpha$  and  $\mathbf{b}$ 
4: Select activation function  $h(x)$ 
5:  $S_0 = \{(P_k, c_k) | k = 1, 2, \dots, K_0\}$  is a little part of S
6:  $\mathbf{H}_0 = [h(\alpha \cdot P_1 + \mathbf{b}), \dots, h(\alpha \cdot P_{K_0} + \mathbf{b})]$ 
7:  $\beta_0 = \mathbf{C}_0 (\mathbf{H}_0^T \mathbf{H}_0)^{-1} \mathbf{H}_0^T$ 
8: Step 2. Continuous learning
9:  $i = 1$ 
10:  $\mathbf{P} \mathbf{h}_0 = (\mathbf{H}_0^T \mathbf{H}_0)^{-1}$ 
11: for  $i$  that satisfies  $(i \times K_0) \leq K$  do
12:  $S_i = \{(P_k, c_k) | k = (i-1) \times K_0 + 1, \dots, i \times K_0\}$ 
13:  $\mathbf{H}_i = [h(\alpha \cdot P_{(i-1) \times K_0 + 1} + \mathbf{b}), \dots, h(\alpha \cdot P_{i \times K_0} + \mathbf{b})]$ 
14:  $\mathbf{P} \mathbf{h}_i = \mathbf{P} \mathbf{h}_{i-1} - \mathbf{P} \mathbf{h}_{i-1} \mathbf{H}_i^T (\mathbf{I} + \mathbf{H}_i \mathbf{P} \mathbf{h}_{i-1} \mathbf{H}_i^T)^{-1} \mathbf{H}_i^T \mathbf{P} \mathbf{h}_{i-1}$  [25]
15:  $\beta_i = \beta_{i-1} + \mathbf{P} \mathbf{h}_i \mathbf{H}_i^T (\mathbf{C}_i - \beta_{i-1} \mathbf{H}_i)$  [25]
16:  $i = i + 1$ 
17: end for
18: Step 3. Fingerprinting positioning
19: Input:  $P_k = [P_{jk} \quad P_{(j+1)k} \quad P_{(i+1)k} \quad P_{(i+1)(j+1)k}]^T$ 
20:  $LEDID(1 \sim 4)$ 
21: for  $ledid$  in  $LEDID(1 \sim 4)$  do
22: search  $(X_{ij}, Y_{ij}, 0)$ 
23: end for
24:  $\hat{c}_k = \beta \cdot h(\alpha \cdot P_k + \mathbf{b})$ 
25: output  $\leftarrow \hat{c}_k + [X_{ij}, Y_{ij}, 0]^T$ 

```

FIGURE 4. The algorithm of VLP system based on ELM.

collection, and it will not affect the positioning accuracy. The VLP system based on ELM is divided into 3 steps, as shown in Algorithm 1 in Fig. 4.

III. SIMULATION AND ANALYSIS

A. INDOOR 3-D POSITIONING SIMULATION MODEL

Simulation experiments on the established ELM for VLP using fingerprinting model is conducted to test the stability and accuracy of the algorithm. As shown in Fig. 2(d), four LEDs located on the ceiling in the simulation experiment. The 3D visible light fingerprinting positioning database is generated by the VLP kernel. The parameters used for the 3-D indoor VLP system using ELM and fingerprinting are shown in Table 1. The ELM model needs to be trained before positioning estimation. It is easy to obtain a large amount of data through simulation, but in the actual process, data sampling is very difficult, especially when the data size reaches

TABLE 1. Simulation parameters of the visible light fingerprint positioning kernel.

Parameter	Value
Size of the VLP kernel (length×width×height) /m	2 m×2 m×3 m
Power of each LED /W	9 W
Position of the four LEDs /m	$LED_{11}(0, 0, 3)$
	$LED_{12}(0, 2, 3)$
	$LED_{21}(2, 0, 3)$
	$LED_{22}(2, 2, 3)$
The number of sampling dots of fingerprint database [K]	10000/20000/30000 /40000/50000
Height of the receiver /m	0 to 2.5
The FOV of the transmitters /deg	60
The FOV of the receiver /deg	70
The diameter of the PD/mm	14 mm
The photodiode responsivity /A·W ⁻¹	0.35
The gain of optical filter [T(ψ_{ijk})]	1.0
The gain of optical concentrator [G(ψ_{ijk})]	1.0
Initial training database size K_0	50
Number of ELM Hidden Layer Nodes \tilde{K}	21
Activation function $h(x)$	Sigmoid function

10,000 or even 100,000. Therefore, we chose 10000, 20000, 30000, 40000, and 50000 as training data sizes respectively to compare their effect on training time and positioning accuracy. In our experiment, the number of ELM Hidden Layer Nodes \tilde{K} is set to 21.

Before carrying out three-dimensional positioning, the fingerprint database needs to be trained. We need the computer’s computational load to be as small as possible. One of the important points is the size of the fingerprint database. As shown in Fig. 5 (a) and (b), when the number of sampling dots of fingerprint database increase from 10000 to 50000, the training time increases rapidly while the average positioning error does not drop significantly. Although the larger the fingerprint database, the higher the positioning accuracy, but the excessive fingerprint database will only increase the difficulty of data collection and waste computing resources without significantly improving the positioning accuracy. Therefore, in the following experiments, we set the fingerprint database density to 10000/12 m³.

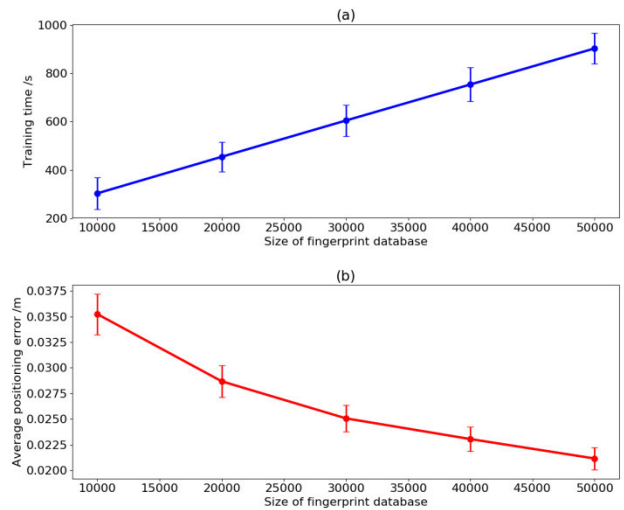


FIGURE 5. The time and error of ELM training fingerprint database.

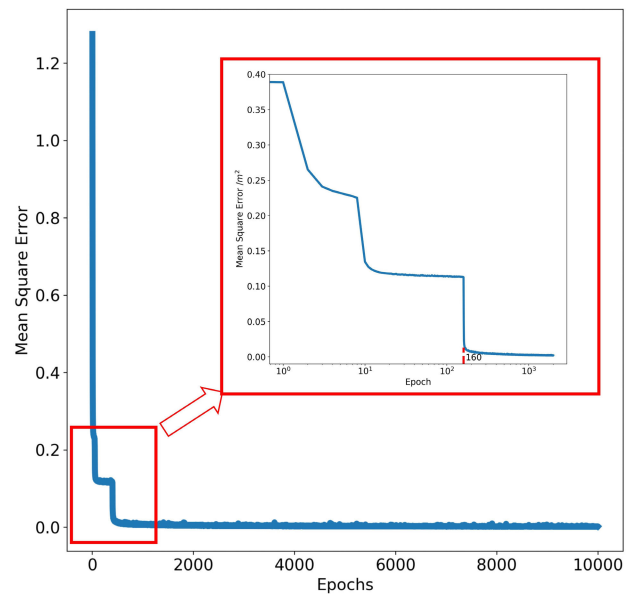


FIGURE 6. Mean square error of the training epochs.

The Mean Square Error (MSE) [26] can serve as the loss function, that is defined as

$$MSE = \frac{1}{K} \sum_{k=1}^K [(x_k - \hat{x}_k)^2 + (y_k - \hat{y}_k)^2 + (z_k - \hat{z}_k)^2] \quad (14)$$

The behavior of MSE in different training epochs is displayed in Fig. 6. When the epoch reach 160, the MSE is basically close to 0.

B. SIMULATION RESULTS AND ANALYSIS

In order to verify the superiority of ELM for 3D visible light fingerprinting positioning, a simulated experiment is conducted about the positioning accuracy of ELM, KNN, and SVM algorithms, respectively. As shown in Fig. 7 (a), (b), and (c), We can intuitively see the effect of

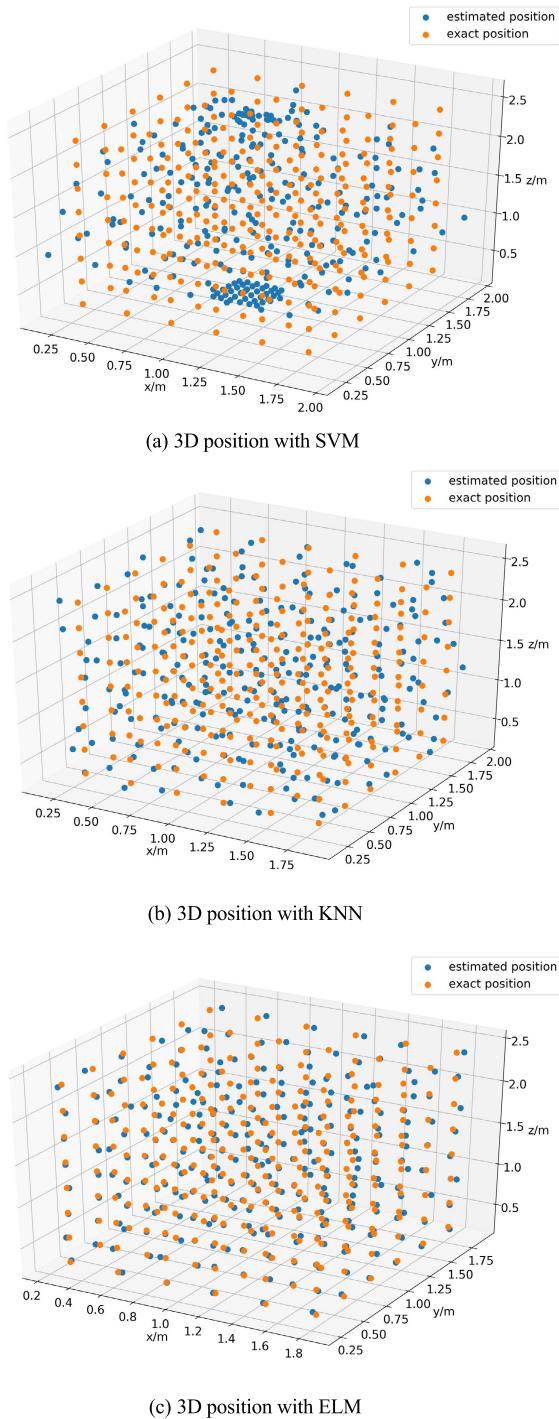


FIGURE 7. The distribution of three-dimensional positioning. Orange points are the exact positions and the blue point are the estimated 3-D position. (a) Represents the 3-D position with SVM, (b) represents the 3-D position with KNN, (c) represents the 3-D position with ELM.

three algorithms for 3D visible light fingerprinting position. Among them, ELM has the best positioning effect. No matter where it is located, positioning using ELM is closer to the real point.

We can get this conclusion more accurately from the 3-D positioning error cumulative distribution function (CDF) [27]

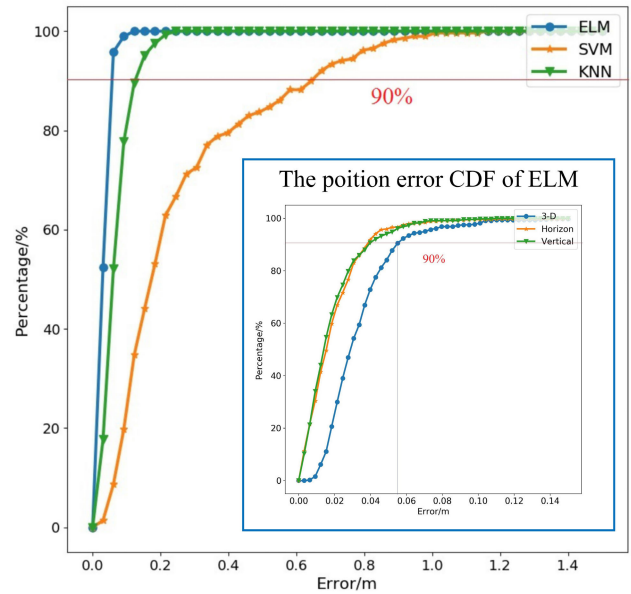


FIGURE 8. Mean square error of the training epochs.

TABLE 2. Computing resources and positioning error comparison of ELM, KNN and SVM.

Parameter	ELM	KNN	SVM
average training time/s	903	0.2	2290
average positioning time/m	0.469	7.478	4.976
average positioning error/m	0.0211	0.0439	0.231

curves in Fig. 8. VLP system based on ELM performs better than KNN and SVM. If 90% of the test points are considered to be acceptable, the 3-D position error CDF curve in Fig. 8 shows that the test points have a maximum 3-D position error of 0.055 m, which proves the VLP system based on ELM performs very well in simulated environment. As shown in TABLE 2, ELM has the shortest positioning time and the lowest positioning error. Though VLP system based on ELM training time is not the shortest, its excellent positioning time and positioning accuracy make it more suitable for VLP system than KNN and SVM.

The whole simulation result of 3-D VLP system based on ELM and fingerprinting is discussed in the Fig. 9. The six figures show that the modified ELM for VLP using fingerprinting works accurately, and their position error are all smaller than 0.07 m. The resolution of the test positions is 0.3 m with height from 0.3 m to 1.8 m in the room and 216 positions are included. All of them are respectively shown in Fig. 9 (a) to (f) for readers, where the solid green points represent the estimated position and the solid red points represent the exact position of the tested points. The proposed positioning system works very good in the whole room in the simulation experiment.

As shown in Fig. 10, the orange line represents the random trajectory and the blue point represent the estimated position

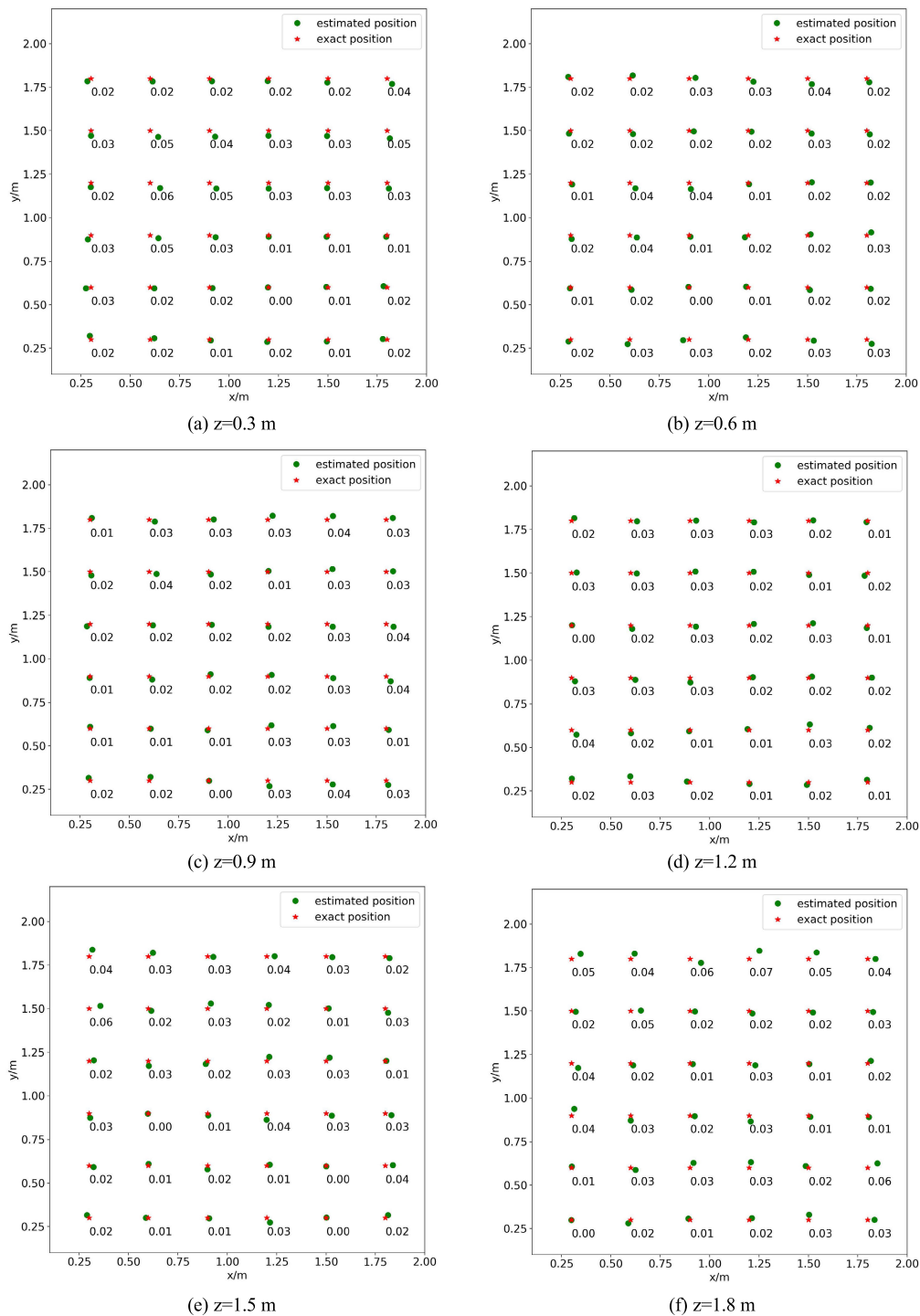


FIGURE 9. Estimated position and 3-D positioning error of the simulated experiment with different height.

of the trajectory using the VLP system based on ELM. From Fig. 10, we can intuitively see that the proposed system has good trajectory tracking effect. In order to further present the positioning effect of the system, the average positioning error is plotted as a function of height in Fig. 11. It can be seen that the average positioning error will increase as the height increases higher than 1.2 m. This is because as the height

increases, the angle ψ_{ijk} between PD and LED increases, and the accuracy of the measurement decreases.

IV. EXPERIMENTS IN REAL ENVIRONMENT AND RESULT

A. EXPERIMENT DESIGN

The data acquisition circuit structure of the three-dimensional VLP system based on ELM is shown in Fig. 12. The computer

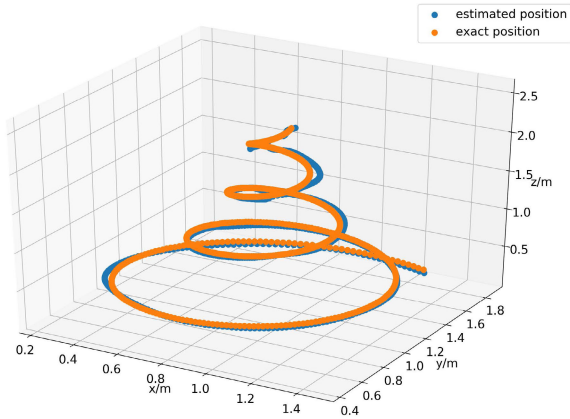


FIGURE 10. 3-D estimated positioning in trajectory tracking using VLP system based on ELM.

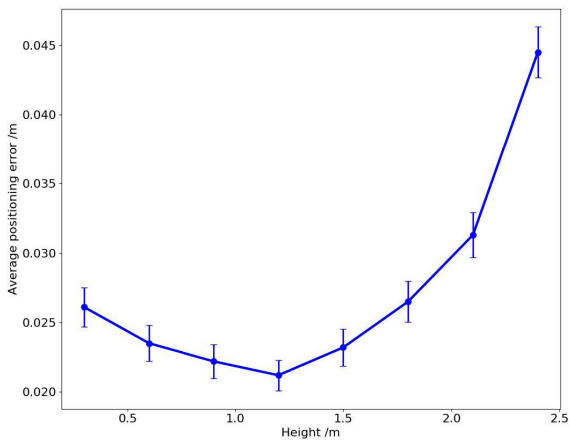


FIGURE 11. Average positioning error of the experiment with different height.

at the transmitting part controls the LED through the serial port, transmits the information and the position ID of the LED. The STM32F407ZG receives the data from the computer and sends data to the LED driving circuit through the I/O port. The driving circuit controls the LEDs. The PD at the receiving part receives the LED signal, and after passing through the first stage amplifier circuit and the second stage amplifier circuit, the STM32F407ZG acquires the ADC measurement and obtains the RSSI value. At the same time, the amplified signal passes through the comparator and enters the STM32F407ZG through the I/O port, performing demodulation and decoding to obtain the LED's position ID.

Visible Light Fingerprint Positioning Kernel Platform Setup: The experiment in real environment is established to verify the practicality and feasibility of the VLP kernel and accuracy of the proposed positioning algorithm. The experimental platform of VLP system based on ELM is shown in Fig. 14 (length is 1.1 m, width is 0.9 m, height is 1.8 m). Four LEDs (pattern: Keced, KC-CBF09, white: 6000 K, power: 9 W) as positioning base station are installed at the top four corners. The PD circuit board of receiving part

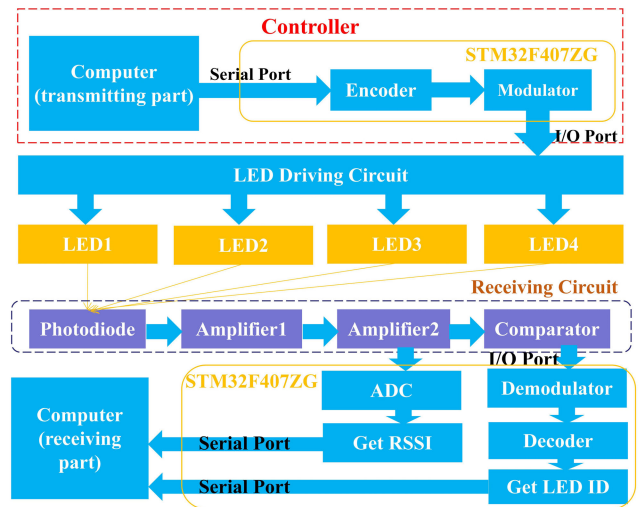


FIGURE 12. The data acquisition circuit structure of the three-dimensional positioning system.

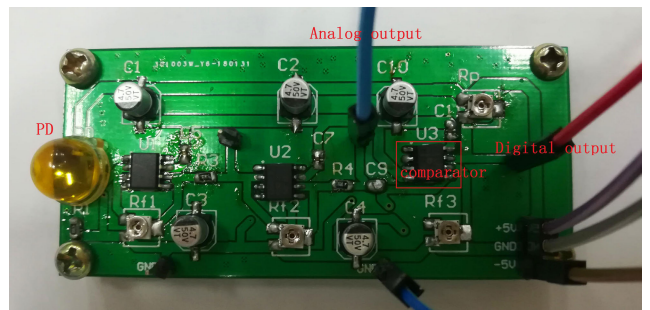


FIGURE 13. The PD circuit board of receiving part.

can be seen in Fig. 13, which includes a digital output and an analog output. The receiver samples the voltage through analog output after the second stage amplifier circuit with an ADC. At the same time, STM32F407 can get the LED ID by acquiring digital output signal of the comparator and decoding by CDMA [13]. The regenerated electrical signal is uploaded to the PC for further processing.

B. RESULTS AND ANALYSIS

Implementation of the proposed three-dimensional positioning algorithm using python3.5, the algorithm runs in Ubuntu16.04. Time spent on each positioning is 0.00177 s, including the time that the signal flows through the receiving circuit, the time of serial communication and the time of algorithm running. We collected 1,200 sets of data for establishing a fingerprint database and trained the fingerprint database using ELM algorithm. In the experiment, there are 24 evenly distributed test points at the height of 0.25 m, 0.50 m, 0.75 m, 1.00 m, 1.25 m and 1.50 m. The positioning results are shown in Fig.15 and Fig. 18. To directly present the result of 3-D positioning using the VLP system based on ELM in real world, the CDF curves of horizon positioning error, vertical positioning error and 3-D positioning error are shown in Fig. 16. From the CDF curve shown in Fig. 16, 90%

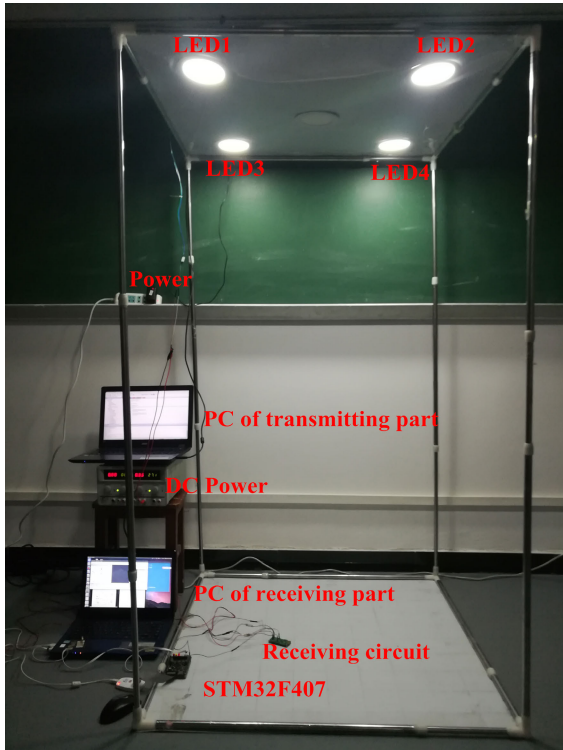


FIGURE 14. Experimental platform of VLP system using fingerprinting and ELM.

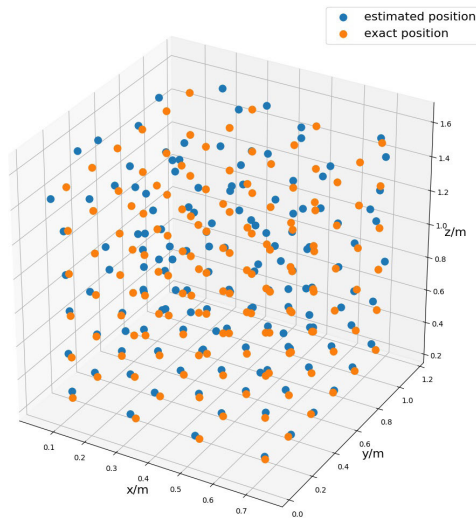


FIGURE 15. Three-dimensional positioning effect of ELM in real world.

of the test points realize a positioning accuracy of 0.08 m. As we can see from Fig.17 and Fig. 18, when the height is 0.25 m, the average error is smaller than 0.025 m and the maximum error is 0.04 m; when the height is 0.50 m, the average error is smaller than 0.020 m and the maximum error is 0.03 m; when the height is 0.75 m, the average error is smaller than 0.0225 m and the maximum error is 0.04 m; when the height is 1.00 m, the average error is smaller than 0.0275 m and the maximum error is 0.07 m; when the height is 1.25 m, the average error is smaller than 0.0375 m and the maximum error is 0.08 m; when the height is 1.50 m,

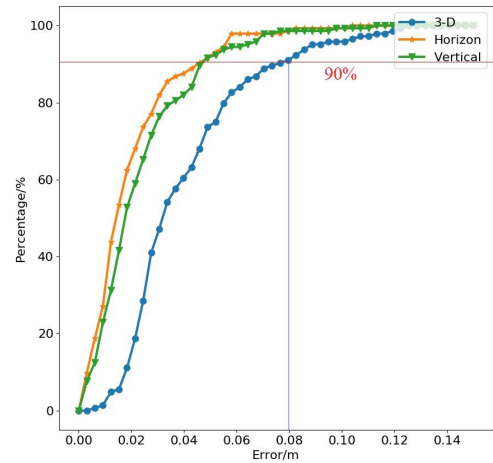


FIGURE 16. The cumulative distribution function (CDF) curves of positioning error in real world.

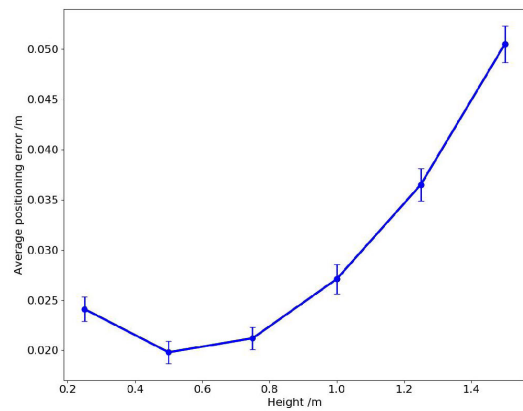


FIGURE 17. Average positioning error of the experiment with different height in real world.

TABLE 3. Accuracy and time performance for different methods.

Methods	Running Environment	Input Nodes	Tra. Time	Error Dist.
K-Nearest Neighbor	-	N	-	≤ 7 cm
four-layer neural network	3.4 GHz/32 GB, Matlab	16 (mutative)	880.8 4 s	≤ 0.4 mm (99%)
Ours	2.6 GHz/8 GB Tensorflow1.4	4 (constant-ant)	903 s	≤ 0.0525 cm (average)
positioning time 0.000469 s				

the average error is smaller than 0.0525 m and the maximum error is 0.10 m. It can be concluded that the VLP system based on ELM works well for 3-D positioning.

VLP Kernel Study: We proposed the VLP kernel to reduce the size of the fingerprint database. In the simulation,

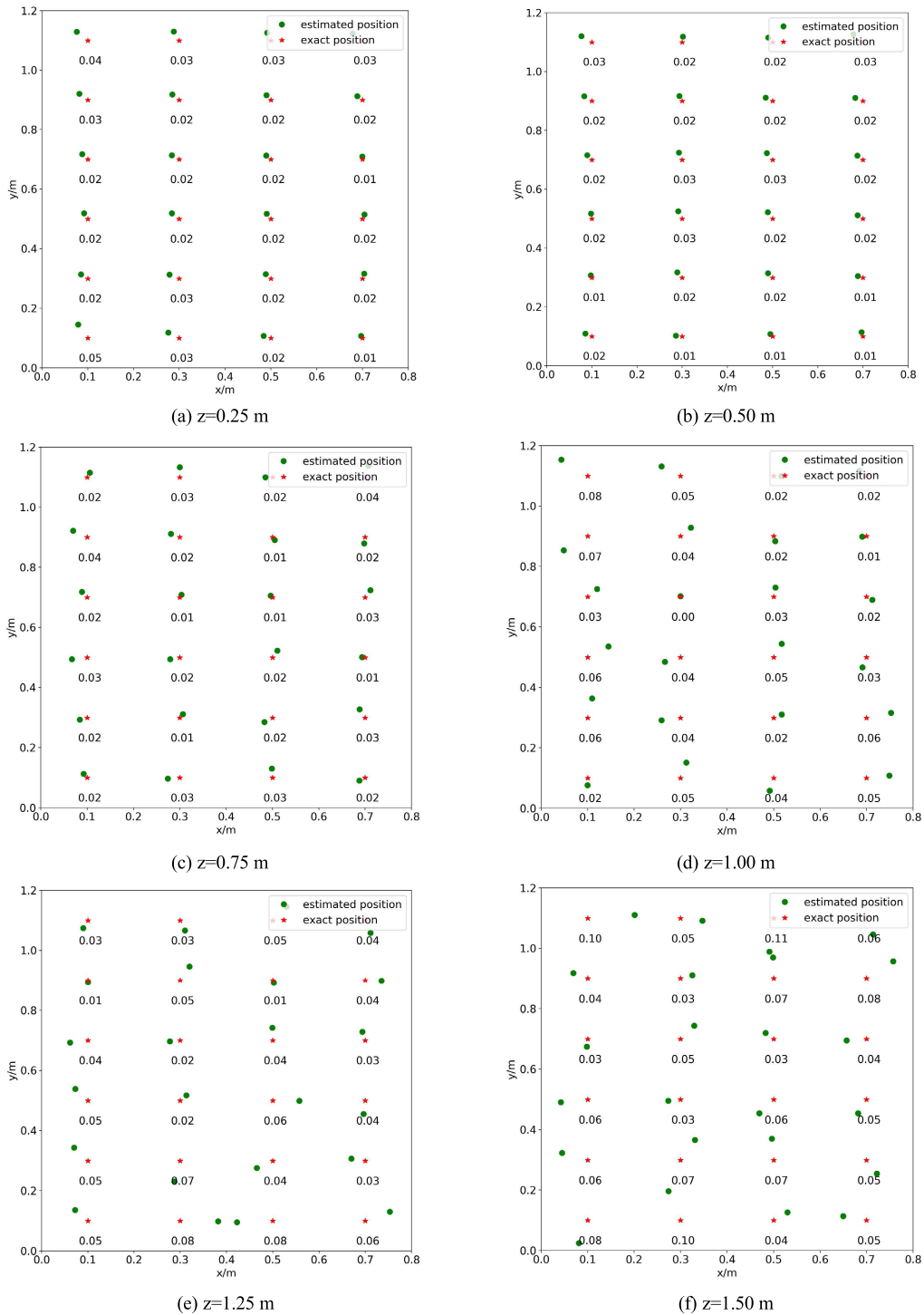


FIGURE 18. Estimated 3-D position of the experiment in real world.

we supposed that the VLP kernel = 2 m × 2 m × 3 m. Compared with four-layer neural network proposed by Alonso-González *et al.* [28], the number of LEDs used in our system is 9/16 of their, when the indoor area is the same. In actual robot or drone positioning, the difference between 4mm and 5cm is not large. However, positioning time is more likely to affect their work. At each

positioning execution, the proposed VLP system based ELM only need to process 28 nodes (4+21+3), whereas their four-layer neural network has to process more than 129 nodes (16+80+30+3). Therefore, it can be estimated that the proposed VLP system is much smaller in positioning time than four-layer neural network, as can be appreciated in Table 3.

TABLE 4. Algorithm running environment.

Parameter	Value
Computer brand	ASUS
RAM	8 GB
CPU	2.6GHz
Tensorflow	1.4
Computer system	Ubuntu16.04

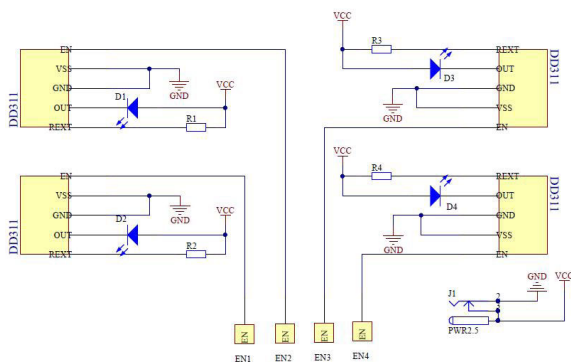


FIGURE 19. The LED driving circuit of transmitting part.

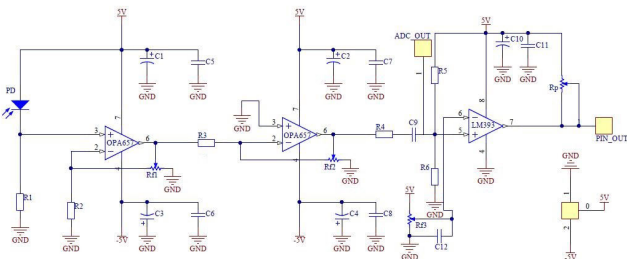


FIGURE 20. The photodiode circuit of receiving part.

V. CONCLUSION AND FUTURE WORKS

In order to make indoor visible light fingerprint positioning can be applied to scenes with large-scale LEDs, this paper proposed a VLP system that firstly split the large indoor positioning environment into regular VLP kernels and then used fingerprinting and ELM algorithm for real-time positioning and less positioning error. In the simulation experiment, the average positioning time is 0.000469 s and the average 3-D positioning error is 0.0211 m. In the experiment in real world, the average positioning time is 0.00177 s and the average 3-D positioning error is 0.0365 m. Both the simulation and the experiment results show that the proposed VLP system achieves real-time 3-D positioning and much less positioning error, which demonstrates the system proposed is suitable for indoor robot positioning, UAV positioning and other indoor scenes that require real-time positioning.

The three-dimensional VLP system supposed the receiver is parallel to the ceiling. However, in the actual working

environment, the VLP system will tilt the receiver due to movement, rotation, etc. Further work is needed to measure device rotation or tilt while tracking and then calibrate the fingerprinting database.

APPENDIX

A. HARDWARE AND SOFTWARE TO RUN ELM

See Table 4.

B. CIRCUIT DESIGN

See Figs. 19 and 20.

ACKNOWLEDGMENT

(Yirong Chen and Weipeng Guan are co-first authors.) Their contributions to the paper are consistent and their ranking is based solely on the first letter of the last name.

REFERENCES

- [1] P. H. Pathak, X. Feng, P. Hu, and P. Mohapatra, "Visible light communication, networking, and sensing: A survey, potential and challenges," *IEEE Commun. Surveys Tuts.*, vol. 17, no. 4, pp. 2047–2077, 4th. Quart., 2015, doi: 10.1109/COMST.2015.2476474.
- [2] A. Yassin, Y. Nasser, M. Awad, A. Al-Dubai, R. Liu, C. Yuen, R. Raulefs, and E. Aboutanios, "Recent advances in indoor localization: A survey on theoretical approaches and applications," *IEEE Commun. Surveys Tuts.*, vol. 19, no. 2, pp. 1327–1346, 2nd Quart., 2016, doi: 10.1109/COMST.2016.2632427.
- [3] N. Ul Hassan, A. Naeem, M. A. Pasha, T. Jadoon, and C. Yuen, "Indoor positioning using visible LED lights: A survey," *ACM Comput. Surv.*, vol. 48, no. 2, Nov. 2015, Art. no. 20, doi: 10.1145/2835376.
- [4] S. Hann, J.-H. Kim, S.-Y. Jung, and C.-S. Park, "White LED ceiling lights positioning systems for optical wireless indoor applications," in *Proc. 36th Eur. Conf. Exhib. Opt. Commun. (ECOC)*, Nov. 2010, pp. 1–3, doi: 10.1109/ECOC.2010.5621490.
- [5] A. Naz, H. M. Asif, T. Umer, and B.-S. Kim, "PDOA based indoor positioning using visible light communication," *IEEE Access*, vol. 6, pp. 7557–7564, 2018.
- [6] L.-C. Chen and J.-K. Lain, "Two-dimensional indoor visible light positioning using smartphone image sensor," in *Proc. IEEE Int. Conf. Consum. Electron.-Taiwan (ICCE-TW)*, May 2018, pp. 2575–8284, doi: 10.1109/ICCE-China.2018.8448675.
- [7] M. F. Keskin, S. Gezici, and O. Arikan, "Direct and two-step positioning in visible light systems," *IEEE Trans. Commun.*, vol. 66, no. 1, pp. 239–254, Jan. 2018, doi: 10.1109/TCOMM.2017.2757936.
- [8] Y. Li, Z. Ghassemlooy, X. Tang, B. Lin, and Y. Zhang, "A VLC smartphone camera based indoor positioning system," *IEEE Photon. Technol. Lett.*, vol. 30, no. 13, pp. 1171–1174, Jul. 1, 2018, doi: 10.1109/LPT.2018.2834930.
- [9] M. Yoshino, S. Haruyama, and M. Nakagawa, "High-accuracy positioning system using visible LED lights and image sensor," in *Proc. IEEE Radio Wireless Symp.*, Jan. 2008, pp. 439–442, doi: 10.1109/RWS.2008.4463523.
- [10] S. H. Yang, H. S. Kim, Y. H. Son, and S. K. Han, "Three-dimensional visible light indoor localization using AOA and RSS with multiple optical receivers," *J. Lightw. Technol.*, vol. 32, no. 14, pp. 2480–2485, Jul. 15, 2014.
- [11] Y. Cai, W. Guan, Y. Wu, C. Xie, Y. Chen, and L. Fang, "Indoor high precision three-dimensional positioning system based on visible light communication using particle swarm optimization," *IEEE Photon. J.*, vol. 9, no. 6, pp. 1–20, Dec. 2017, doi: 10.1109/JPHOT.2017.2771828.
- [12] H. Steendam, "A 3-D positioning algorithm for AOA-based VLP with an aperture-based receiver," *IEEE J. Sel. Areas Commun.*, vol. 36, no. 1, pp. 23–33, Jan. 2018, doi: 10.1109/JSAC.2017.2774478.
- [13] H. Chen, W. Guan, S. Li, and Y. Wu, "Indoor high precision three-dimensional positioning system based on visible light communication using modified genetic algorithm," *Opt. Commun.*, vol. 413, pp. 103–120, Apr. 2018, doi: 10.1016/j.optcom.2017.12.045.

- [14] D. Konings, B. Parr, F. Alam, and E. M.-K. Lai, "Falcon: Fused application of light based positioning coupled with onboard network localization," *IEEE Access*, vol. 6, pp. 36155–36167, 2018, doi: [10.1109/ACCESS.2018.2847314](https://doi.org/10.1109/ACCESS.2018.2847314).
- [15] B. Zhu, J. Cheng, Y. Wang, J. Yan, and J. Wang, "Three-dimensional VLC positioning based on angle difference of arrival with arbitrary tilting angle of receiver," *IEEE J. Sel. Areas Commun.*, vol. 36, no. 1, pp. 8–22, Jan. 2018, doi: [10.1109/JSAC.2017.2774435](https://doi.org/10.1109/JSAC.2017.2774435).
- [16] M. Xu, W. Xia, Z. Jia, Y. Zhu, and L. Shen, "A VLC-based 3-D indoor positioning system using fingerprinting and K-nearest neighbor," in *Proc. Veh. Technol. Conf. (VTC Spring)*, Nov. 2017, pp. 1–5, doi: [10.1109/VTC-Spring.2017.8108345](https://doi.org/10.1109/VTC-Spring.2017.8108345).
- [17] S. Berchtold, C. Böhm, D. A. Keim, and H.-P. Kriegel, "A cost model for nearest neighbor search in high-dimensional data space," in *Proc. 16th ACM SIGACT-SIGMOD-SIGART Symp. Princ. Database Syst.*, 1997, pp. 78–86, doi: [10.1145/263661.263671](https://doi.org/10.1145/263661.263671).
- [18] K. Kaemarungsi and P. Krishnamurthy, "Modeling of indoor positioning systems based on location fingerprinting," in *Proc. 23rd Annu. Joint Conf. IEEE Comput. Commun. Soc. (INFOCOM)*, Mar. 2004, pp. 1012–1022, doi: [10.1109/INFCOM.2004.1356988](https://doi.org/10.1109/INFCOM.2004.1356988).
- [19] T. Wigren, "Adaptive enhanced cell-ID fingerprinting localization by clustering of precise position measurements," *IEEE Trans. Veh. Technol.*, vol. 56, no. 5, pp. 3199–3209, Sep. 2007, doi: [10.1109/TVT.2007.900400](https://doi.org/10.1109/TVT.2007.900400).
- [20] G.-B. Huang, H. Zhou, X. Ding, and R. Zhang, "Extreme learning machine for regression and multiclass classification," *IEEE Trans. Syst., Man, Cybern. B, Cybern.*, vol. 42, no. 2, pp. 513–529, Apr. 2012, doi: [10.1109/TSMCB.2011.2168604](https://doi.org/10.1109/TSMCB.2011.2168604).
- [21] G.-B. Huang, Q.-Y. Zhu, and C.-K. Siew, "Extreme learning machine: Theory and applications," *Neurocomputing*, vol. 70, nos. 1–3, pp. 489–501, 2006, doi: [10.1016/j.neucom.2005.12.126](https://doi.org/10.1016/j.neucom.2005.12.126).
- [22] G.-B. Huang, Q.-Y. Zhu, and C.-K. Siew, "Extreme learning machine: A new learning scheme of feedforward neural networks," in *Proc. IEEE Int. Joint Conf. Neural Netw.*, Jan. 2004, pp. 985–990, doi: [10.1109/IJCNN.2004.1380068](https://doi.org/10.1109/IJCNN.2004.1380068).
- [23] Y. Miche, A. Sorjamaa, P. Bas, O. Simula, C. Jutten, and A. Lendasse, "OP-ELM: Optimally pruned extreme learning machine," *IEEE Trans. Neural Netw.*, vol. 21, no. 1, pp. 158–162, Jan. 2010, doi: [10.1109/TNN.2009.2036259](https://doi.org/10.1109/TNN.2009.2036259).
- [24] T. Komine and M. Nakagawa, "Fundamental analysis for visible-light communication system using LED lights," *IEEE Trans. Consum. Electron.*, vol. 50, no. 1, pp. 100–107, Feb. 2004, doi: [10.1109/TCE.2004.1277847](https://doi.org/10.1109/TCE.2004.1277847).
- [25] Y. Sun, Y. Yuan, and G. Wang, "An OS-ELM based distributed ensemble classification framework in P2P networks," *Neurocomputing*, vol. 74, no. 16, pp. 2438–2443, Sep. 2011, doi: [10.1016/j.neucom.2010.12.040](https://doi.org/10.1016/j.neucom.2010.12.040).
- [26] C. M. Theobald, "Generalizations of mean square error applied to ridge regression," *J. Roy. Stat. Soc. B (Methodol.)*, vol. 36, no. 1, pp. 103–106, 1974, doi: [10.2307/2984775](https://doi.org/10.2307/2984775).
- [27] M.-H. Chuna, S.-J. Han, and N.-I. Tak, "An uncertainty importance measure using a distance metric for the change in a cumulative distribution function," *Rel. Eng. Syst. Saf.*, vol. 70, no. 3, pp. 313–321, Dec. 2000, doi: [10.1016/S0951-8320\(00\)00068-5](https://doi.org/10.1016/S0951-8320(00)00068-5).
- [28] I. Alonso-González, D. Sánchez-Rodríguez, C. Ley-Bosch, and M. A. Quintana-Suárez, "Discrete indoor three-dimensional localization system based on neural networks using visible light communication," *Sensors*, vol. 18, no. 4, p. 1040, Mar. 2018, doi: [10.3390/s18041040](https://doi.org/10.3390/s18041040).



YIRONG CHEN received the B.S. degree in electronic science and technology from the South China University of Technology, China, in 2019. He is currently pursuing the Ph.D. degree with the School of Electronic and Information Technology, South China University of Technology. His research interests include visible light communications, natural language processing, and emotional calculation. He is also a Journal Reviewer of the IEEE PHOTONICS JOURNAL and IEEE ACCESS.



WEIPENG GUAN received the B.E. degree from the Electronic Science and Technology Department (Electronic Materials and Components Department) and the M.S. degree from the Control Theory and Control Engineering Department, South China University of Technology, Guangzhou, China. He is currently pursuing the Ph.D. degree with the Department of Information Engineering, The Chinese University of Hong Kong, Hong Kong. His research is focused on visible light wireless communication technology and visible light positioning technology.



JINGYI LI was born in Gansu, China, in 1998. He is currently pursuing the B.E. degree with the School of Automation Science and Technology, South China University of Technology (SCUT), Guangzhou, China. He joined R&C Academic Studio, SCUT, when he was a Sophomore. His research interests are visible light communications, machine vision, and optimization and edge computing.



HONGZHAN SONG was born in Jiangxi, China, in 2001. She is currently pursuing the B.E. degree with the School of Automation Science and Engineering, South China University of Technology. She is also focused on the research of mobile robots and visible light positioning.

• • •